Journal of Alloys and Compounds 488 (2009) 284–290

Contents lists available at ScienceDirect

Journal of Alloys and Compounds

journal homepage: www.elsevier.com/locate/jallcom

Formation of composite nanomaterial $MnPS_3$ layered structure intercalated with pyridine

A.A. El-Meligi[a,b,*], A.M. Al-Saie[b], H. Al-Buflasa[b], M. Bououdina[b]

[a] National Research Centre, Department of Physical Chemistry, Dokki, Cairo, Egypt
[b] University of Bahrain, College of Science, Department of Physics, Manama, Bahrain

ARTICLE INFO

Article history:
Received 4 August 2009
Accepted 22 August 2009
Available online 27 August 2009

Keywords:
Nanomaterial
Pyridine
Intercalation
X-ray diffraction
Crystal structure

ABSTRACT

Intercalated compound of pyridine into layered $MnPS_3$ has been synthesized and characterized by X-ray powder diffraction (XRD), Infrared (IR) and Scanning Electron Microscopy connected with chemical analysis (SEM-EDEX). It is found that leaving the intercalated compound in open atmosphere for a number of days influences the existing phase and the arranged orientation of the pyridine in the interlayer gap (6.4 Å) of the $MnPS_3$ lattice. The estimated crystallite size varied with leaving the intercalated sample in open atmosphere and reached a lowest value of about 26 nm. Three phases coexisted together as confirmed by XRD: the 0 0 1′ phase (with lattice spacing 9.6 Å); the 0 0 1″ phase (with lattice spacing of 10.7 Å); and other phase with lattice spacing of 7.3 Å. The phase transformation occurs between the two phases of lattice spacing 10.7 Å and 9.6 Å. Before and after intercalation, the $MnPS_3$ exhibits paramagnetic behaviour at room temperature.

1. Introduction

MPX_3 materials (M is a transition elements such as Fe, Mn and X = S, Se) with their interesting layered structure have been deeply investigated over the past 20 years. A wide range of guests was known to be intercalated into the MPS_3, such as inorganic, organic cations, organometallic molecules and biomolecules [1–4]. These materials offer different applications, such as rechargeable batteries, catalysts, ferroelectric, non-linear optical and magnetic materials [5–8]. The properties of the layered materials are affected, for example, there is a tangible change in conductivity, optical properties, magnetic properties and superconductivity. This may be ascribed to a simple charge transfer model in which electrons are transferred from the guest species to the host lattice [9–12]. Different mechanisms of intercalation process were proposed. For example, pyridine intercalated in layered materials such as, TaS_2, etc., could not be explained on the basis of the charge transfer model, since the orientation of pyridine molecules in their Van der Waals gap disallows and direct interaction between the nitrogen lone pair and the host lattice [13,14]. The intercalation of pyridinium ions led to the suggestion of different mechanisms [15]. Different phases were resulted due to the intercalation of $MnPS_3$ with pyridinium ions [16]. The appearance of these phases depends on a number of factors, such as, guest position in the interlayer of the host, solvents, stirring period, temperature during intercalation and the temperature during XRD measurements [17,18].

This work aims to study the intercalation of pyridine into layered materials of $MnPS_3$ under specific conditions. The effects of leaving the intercalated compound in open atmosphere on crystal size and phase transformation were investigated. Moreover, to the best of our knowledge; it is the first time to estimate the crystal size during phase transformation in open atmosphere.

2. Experiments

2.1. Synthesis of pure $MnPS_3$

Stoichiometric amounts of high-purity elements (≥99.9%), Mn, P, and S, are mixed to have homogeneous mixture. The reaction of the elements was carried out in an evacuated silica tube at 650 °C for 1 week. These conditions were applied to produce pure material of $MnPS_3$ [16]. The green powder was taken of the sealed silica tube and grinded. The material was indexed and refined as a monoclinic unit cell and space group $C2/m$ with lattice parameters are, $a = 6.08$ Å, $b = 10.53$ Å, $c = 6.8$, and $\beta = 107.2165°$ in agreement with literature [19,20,16]. The lattice parameters were computed by a least-square refinement of the observed reflections.

2.2. Intercalation under specific conditions

The intercalation was carried out by stirring the mixture of 0.15 g of $MnPS_3$ and 5 ml of pyridine in presence of solvents: distilled

* Corresponding author. Fax: +0020233370931.
E-mail address: ael_meligi10@hotmail.com (A.A. El-Meligi).

0925-8388/$ – see front matter © 2009 Elsevier B.V. All rights reserved.
doi:10.1016/j.jallcom.2009.08.106

water and concentrated hydrochloric acid (HCl) for 4 h at 60 °C. Fast stream of nitrogen was bubbled during intercalation. The mixture was stirred by magnetic stirrer at speed 5 (5 × 1000 rpm) till the solution was completely evaporated. After stopping the intercalation process, the powders were filtered off, and washed with water, then dried.

2.3. Characterization techniques

X-ray diffraction (XRD) patterns were recorded on a Philips diffractometer equipped with Cu kα (λ = 1.5418 Å) radiation. Elemental analysis was determined. The indexing and refinement were performed using Topaz Program. The structure was built by using the Atoms Program-Version 5.1. Magnetic measurements were conducted using a vibrating sample magnetometer (VSM) in an applied field of 1000 Oe at room temperature using PMC MicroMag 3900 Model-having a 1 T magnet. The magnetic measurements were performed by filling capsules with certain amount of dried oxide powder. Scanning electron microscopy observations with chemical analysis (SEM-EDEX) were performed to identify changes in the surface topography and to determine the chemical composition in the compounds. The images were performed using ZEISS-ESEM-Hi-Vac mode, the acceleration voltage is 10 kV. Infrared spectra (IR) were recorded using PerkinElmer 1600 FTIR. The IR spectra of the pure and intercalated $MnPS_3$ with pyridine were obtained by mixing about 0.2 mg of the samples with 0.2 g of KBr, and then pellets of the mixture were made under vacuum.

3. Results and discussion

3.1. X-ray powder diffraction

X-ray powder diffraction (XRD) pattern was recorded after stopping experiment and washing the sample with distilled water then dried. The intercalated compound has a general formula, $Mn_{1-x}PS_3(G)_{2x}\cdot(H_2O)_y$, where $MnPS_3$ is the host and G is the guest species (organic or inorganic compound) [13–15]. The 0 0 l phase with the lattice spacing of 6.47 Å is the pristine $MnPS_3$. It is found that three phases appear, as in Fig. 1. The predominant one is the 0 0 1′ phase with lattice spacing of 9.6 Å ($2\theta = 9.225^\circ$), indicating the parallel orientation of the pyridine molecular ring to the $MnPS_3$ layer [16,21]. The 0 0 1″ phase with lattice spacing of 10.7 Å indicates that the pyridine molecular rings are not parallel or perpendicular to the $MnPS_3$ layer [18]. The remaining phase has a lattice spacing of 7.3 Å (denoted as d7 phase). This phase almost coexists with 0 0 l″ phase and disappears with it. It was mentioned that the molecules inserted in the interlayer gap could be parallel, perpendicular and in between these positions [16]. The intercalated phases can be readily indexed in a trigonal unit cell, as indicated in the case of pyridinium ion intercalated with $MnPS_3$ [16]. Based on such indexing, the *c*-axis is extended with the *d*-spacing expansion. With respect to 0 0 1 phase of $MnPS_3$, 0 0 1″ phase expands *d*-spacing by 4.2 Å and *c*-axis by 32.68 Å and 0 0 1′ phase expands *d*-spacing by 3.3 Å and *c*-axis by 29 Å. The presence of HCl as an aggressive solvent has no effect on the crystallinity of the $MnPS_3$. This is an agreement with the results of 4-picoline inserted into the interlayer of $MnPS_3$ in the presence of HCl [17]. There was no deformation or amorphization of the material.

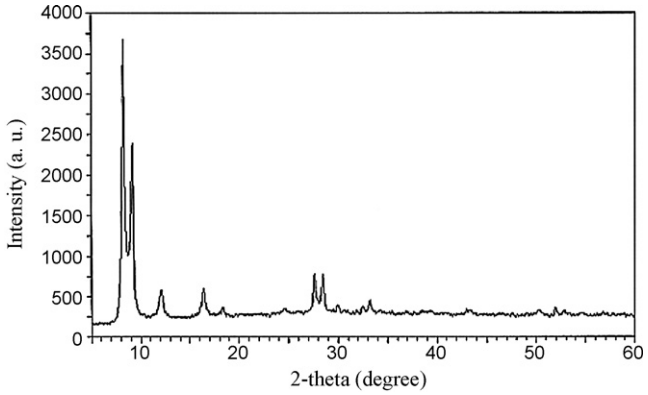

Fig. 2. XRD pattern of pyridine intercalated into $MnPS_3$ layers $[Mn_{1-x}PS_3[pyr_{2x}(H_2O)_y]$ measured after leaving sample (Fig. 1) for 3 h in open air at RT. Three phases are still observed. Phase transformation of 0 0 1′ phase to 0 0 1″ phase.

3.2. Phases transformation in open atmosphere

From the XRD results, it can be seen clearly the phase transformation between 0 0 1″ phase and 0 0 1′ phase. This transformation occurs due to leaving the intercalated compound in open atmosphere at room temperature without any other external effect. It was observed that phase transformation occurred from 0 0 1′ phase to 0 0 1″ phase after leaving the sample in open atmosphere for 3 h (Figs. 1 and 2). As shown in Fig. 3, the 00l′ phase disappears and 0 0 1″ phase is intensified and a complete intercalate is obtained that only contains the 0 0 1″ phase after 1 day in open atmosphere at RT. The 0 0 1″ phase starts to transform into 0 0 1′ phase, as observed in Fig. 4. The XRD pattern was recorded for 36 days in order to follow the phase transformation of 0 0 1″ phase into 0 0 1′ phase. After 26 and 30 days in open atmosphere, it is clear that the 0 0 1″ phase transforms into 0 0 1′ phase and the 0 0 1′ is intensified in the XRD pattern, as shown in Figs. 5 and 6. It is worth to notice that, the

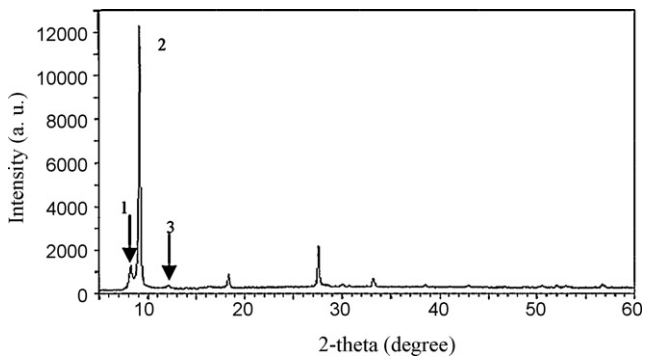

Fig. 1. XRD pattern of pyridine intercalated into $MnPS_3$ layers $[Mn_{1-x}PS_3[pyr_{2x}(H_2O)_y]$ measured after stopping and washing with distilled water. Three phases are presented 0 0 1″ (1), 0 0 1′ (2) and d7 (3).

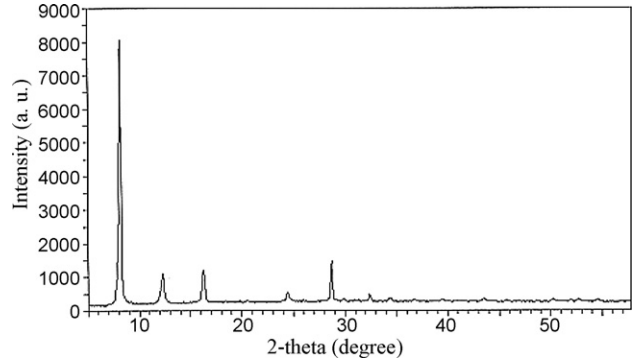

Fig. 3. XRD pattern of pyridine intercalated into $MnPS_3$ layers $[Mn_{1-x}PS_3[pyr_{2x}(H_2O)_y]$ measured after leaving sample (Fig. 2) one day in open air at RT. Complete phase transformation of 0 0 1′ phase to 0 0 1″ phase.

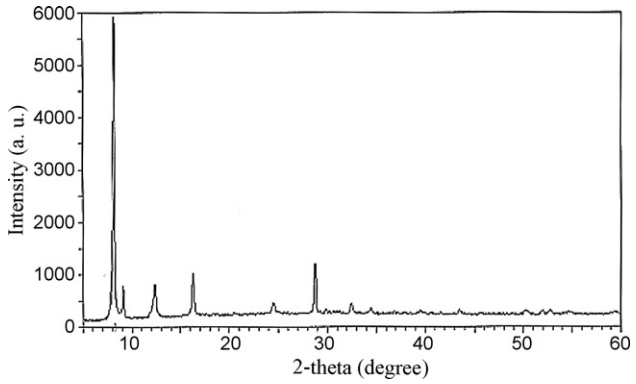

Fig. 4. XRD pattern of pyridine intercalated into $MnPS_3$ layers $[Mn_{1-x}PS_3[pyr_{2x}(H_2O)_y]$ measured after leaving sample (Fig. 3) for two day in open air at RT. Phase transformation starts of 0 0 1″ phase to 0 0 1′ phase.

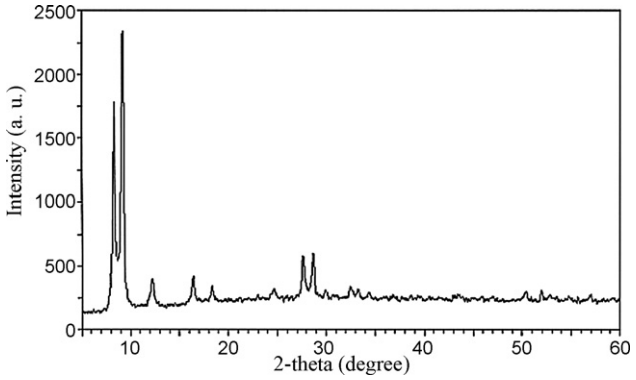

Fig. 5. XRD pattern of pyridine intercalated into $MnPS_3$ layers $[Mn_{1-x}PS_3[pyr_{2x}(H_2O)_y]$ measured after leaving sample (Fig. 4) of for 26 day in open air at RT. Phase transformation continues of 0 0 1″ phase to 0 0 1′ phase.

d7 phase starts to appear with phase transformation of 0 0 1′ phase into 0 0 1″ phase. This means that the d7 phase may be related to the 0 0 1″ phase (as shown in Figs. 2–4, 7, 5 and 6). Moreover, it is observed that after the 0 0 1″ phase becomes predominant, the d7 phase is not affected through 24 days (Figs. 4, 7, 5). It can be proposed that the d7 phase is formed following two considerations: (i) the lattice spacing of $MnPS_3$ is slightly expanded by about 0.9 Å due to the few molecules of pyridine which are inserted into the interlayer gap and (ii) the presence of H_2O vapor, which is evaporated when left in open air and during XRD measurements. A complete phase transformation to 0 0 1′ phase was observed after 36 days in

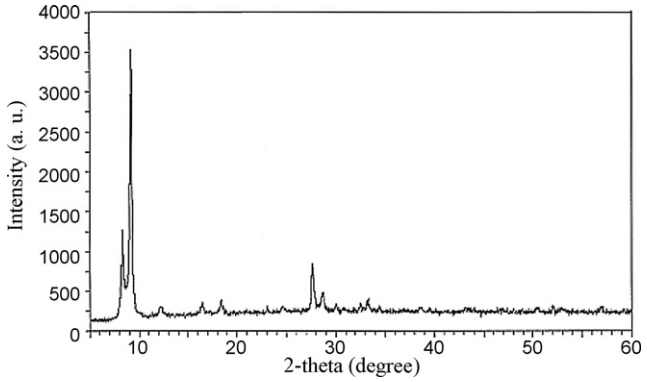

Fig. 6. XRD pattern of pyridine intercalated into $MnPS_3$ layers $[Mn_{1-x}PS_3[pyr_{2x}(H_2O)_y]$ measured after leaving sample (Fig. 5) for 30 day in open air at RT. Phase transformation continues of 0 0 1″ to 0 0 1′ and the 0 0 1′ phase predominated.

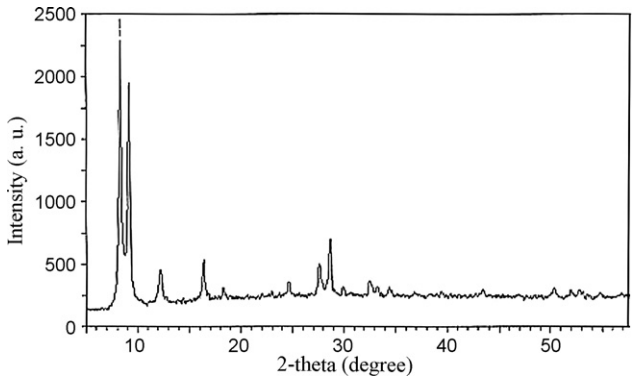

Fig. 7. XRD pattern of pyridine intercalated into $MnPS_3$ layers $[Mn_{1-x}PS_3[pyr_{2x}(H_2O)_y]$ measured after leaving sample (Fig. 6) for 24 day in open air at RT. Phase transformation continues of 0 0 1″ to 0 0 1′.

open atmosphere, as can be seen in Fig. 8. The mechanism of phase transformation to 0 0 1′ phase of pyridine intercalated into interlayer gap of $MnPS_3$ is similar to that of pyridinium ion inserted into $MnPS_3$ [16]. It could be confirmed that the 0 0 1′ phase is the most stable intercalated phase of the $MnPS_3$ compound with pyridine and its derivatives.

3.3. Crystallite size estimation

The crystallite size (CS) and lattice strains (LS) of the 0 0 1″ phase, 0 0 1′ phase and d7 phase, were estimated from peak profile refinements of the XRD patterns, which are recorded during phase's transformation in open atmosphere at room temperature. It is worthy to notice that the crystallite size varies during phase transformation, especially, 0 0 1″ phase into 0 0 1′ phase, as shown in Table 1. As observed, the crystallite size of the pure $MnPS_3$ is about 889 nm. This big crystal size might be due to the fact that after fabrication, the $MnPS_3$ was left inside the sealed tube for about 3 years where crystallites growth might occur. Moreover, the evacuated environment (vacuum) might help in the crystallite size growth. Complete phase transformation into 0 0 1″ phase after leaving the sample for one day in open atmosphere leads to a tremendous decrease in the crystallite size to about 80 nm. The CS is significantly reduced when both phases (0 0 1″ and 0 0 1′) coexist together with nearly similar ratio, as highlighted in Table 1. The largest crystallite size was estimated for 0 0 1′ phase, about 440 nm. This may be due to crystallites agglomeration during phase transformation of 0 0 1″ phase into 0 0 1′ phase, in which the position of the intercalated pyridine would be oriented parallel to the $MnPS_3$ layers [16,17]. The lowest crystallite size was estimated

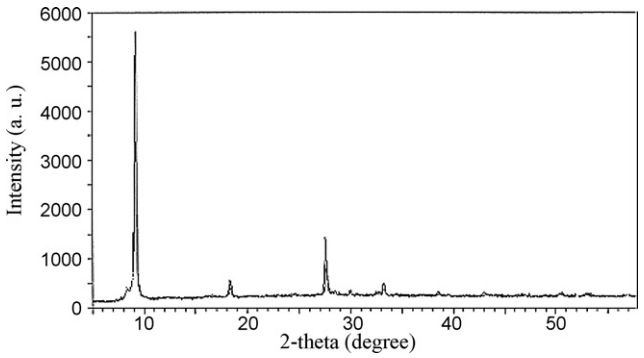

Fig. 8. XRD pattern of pyridine intercalated into $MnPS_3$ layers $[Mn_{1-x}PS_3[pyr_{2x}(H_2O)_y]$ measured after leaving sample (Fig. 7) of for 36 day in open air at RT. Complete phase transformation of 0 0 1″ phase to 0 0 1′ phase.

Table 1
Estimated crystallite size of during phases transformation in open air.

Time in open air	Pure MnPS3 (*d*-spacing = 6.4 Å)		d10 (*d*-spacing = 10.84 Å)		d9 (*d*-spacing = 9.7 Å)		d7 (*d*-spacing = 7.34 Å)	
	CS (nm)	LS (%)	CS (nm)	LS (%)	CS (nm)	LS (%)	CS (nm)	LS (%)
0	889	0.155	–	–	–	–	–	–
1/2 h	–	–	85	1.089	121	0.718	27	1.568
3 h	–	–	30	2.137	24	2.221	27	1.585
1 day	–	–	80	1.054	–	–	34	1.289
2 days	–	–	105	0.883	–	–	32	1.368
7 days	–	–	103	0.886	443	0.343	38	1.204
9 days	–	–	100	0.900	285	0.438	43	1.099
17 days	–	–	103	0.882	199	0.535	41	1.142
21 days	–	–	91.5	0.956	190	0.551	43	1.095
24 days	–	–	39	1.722	38	1.613	29	1.47
26 days	–	–	33	1.99	42	1.491	25	1.648
30 days	–	–	26	2.375	51	1.286	–	–
36 days	–	–	–	–	85	0.905	–	–

N.B. CS is the crystallite size and LS is the lattice strain.

for the d7 phase within the range of 25 up to 43 nm. Generally, the crystallite size growth within the nanosize range can be regarded as the coalescence of small neighboring crystallites due to atomic diffusion or discrete orientation attachment and crystallographically oriented crystallites [22]. In this work, there is orientation of the intercalated guest in the interlayer gap of the $MnPS_3$. Also, the crystallites size variation due to leaving in open atmosphere is similar to the case of the nanocrystallite anatase in which the oriented attachment controlled the crystallites growth [23]. Lattice strain (LS) is greatly affected by the variation of CS. As presented in Table 1, the increase the CS is followed by a decrease of LS and vice versa. Schematic model have been proposed to present phases transformation in open atmosphere, as shown in Fig. 9.

3.4. Proposed intercalation mechanism

The intercalated molecules of pyridine have three positions, perpendicular, inclined (not parallel or perpendicular) and parallel to the $MnPS_3$ layers. This proposition is based on a similar suggested model for pyridinium ion inserted into the interlayer gap of $MnPS_3$ [16]. The pyridinium ions could be in one of these positions. As mentioned, the intercalates have a general formula, $Mn_{1-x}PS_3(G)_{2x}\cdot(H_2O)_y$, where G is the guest ionic species [24–27]. The charge balance of these compounds has been maintained by the loss of one M^{2+} ion from the intralayer region for every two guest ions (G^+) that are inserted and located in the interlayer space. Therefore, it is proposed that pyridine as a guest (G) could be ionized to be G^+. Based on the chemistry of the intercalation, pyridine

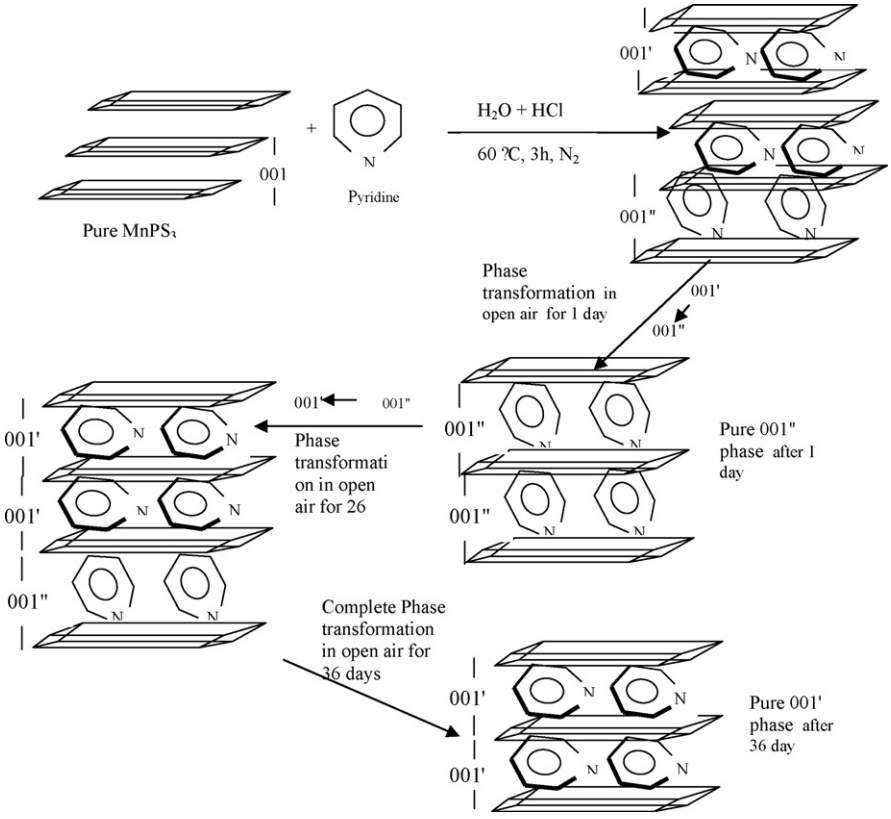

Fig. 9. Proposed schematic intercalation mechanism of pyridine into $MnPS_3$ layers. It is based on the results of the XRD Figs. 1–8. There is a phase transformation of 0 0 1′ phase to 0 0 1′′ phase, then to 0 0 1′ phase due to leaving sample in open air at RT.

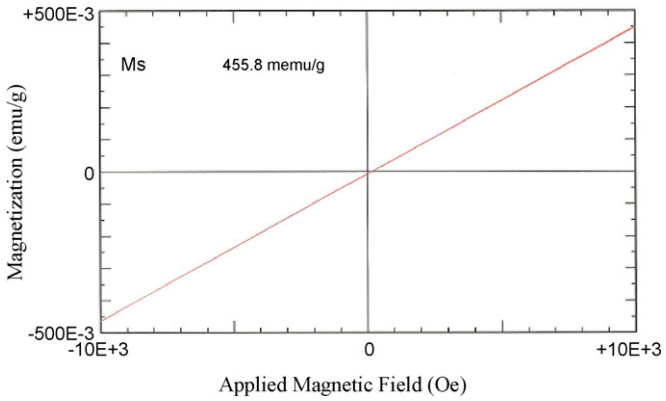

Fig. 10. Magnetization of pure $MnPS_3$.under the effect of applied magnetic field.

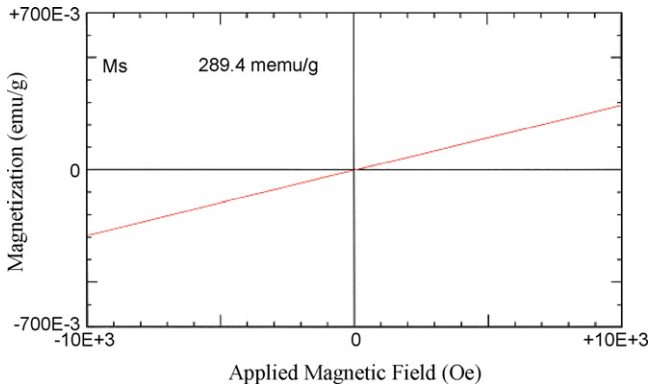

Fig. 11. Magnetization of intercalate compound of pyridine and $MnPS_3$ $[Mn_{1-x}PS_3[pyr_{2x}(H_2O)_y]$.

could convert to pyridinium (pyH^+) and vice versa. The pyH^+ is probably formed by the reaction: pyridine + $H_3O^+ \leftrightarrow pyH^+ + OH^-$ [13,28]. It was stated ammonia intercalating into TaS_2 could be oxidized into ammonium ions solvated by neutral molecules, as well; the pyridine intercalated into TaS_2 has shown the same behaviour [29,30]. EDEX analysis of intercalates reveals that there is always a significant loss of Mn^{2+} cations accompanying the intercalation process, which will be shown vide infra. Also, elemental analysis of intercalates has shown a significant loss of Mn^{2+} cations due to intercalation [13,16,17]. Accordingly, the guest species must be protonated to balance electrical charges of the layered material. The presence of concentrated hydrochloric acid (HCl) is the proton source. Therefore, the intercalation mechanism is based on an ion exchange rather than on an electron transfer. Silipigni et al. [19] proved by using the XPS measurements that binding energy position values obtained in the case of $K_{2x}Mn_{1-x}PS_3$ for the Mn 2p and 3p, S 2p and 2s and P 2p and 2s core levels are very similar to those deduced for $MnPS_3$. This result is in agreement with the intercalation by substitution, which is based on an ion transfer rather than on an electron transfer as indeed happens in the intercalation by reduction [20].

3.5. VSM measurements

Curves of magnetization versus the applied magnetic field were plotted (M–H loop) for the pure $MnPS_3$ before and after intercalation with pyridine. The M–H loop indicates that $MnPS_3$ is paramagnetic. The value of the saturation magnetization (M_s) of $MnPS_3$ per gram is 456 memu/g, as shown in Fig. 10. As mentioned, MPS_3 phases containing some paramagnetic M^{2+} ions and the paramagnetic properties of $MnPS_3$ could be affected by experimental conditions [18]. After intercalation, the M–H curve confirms that the intercalated compound remains paramagnetic, as observed in Figs. 10 and 11. However, the phase transformation has affected the value of Ms. Transformation of 0 0 1″ phase to 0 0 1′ phase decreases the Ms value to 209 memu/g with respect to the Ms of pure $MnPS_3$. Moreover, transformation of 0 0 1′ phase to 0 0 1″ phase (Fig. 2) increases the Ms to a value to 292 memu/g. The presence of 0 0 1″ phase and 0 0 1′ phase together in the XRD pattern leads to a decrease of Ms value to 257 memu/g. The paramagnetic behaviour of intercalated compound may be due to the existence of much more intralayered Mn^{2+} vacancies of the host layer [4]. In fact, magnetic properties of materials are generally influenced by many factors, such as crystallite size, crystal structure, particles surface disorder, morphologies, etc. [31]. The variation of the magnetic properties may be due the effect of magnetic anisotropy [32]. The magnetic anisotropy simply means that the magnetic properties depend on the direction (*hkl* planes) in which they are measured.

3.6. Structure morphology

Structure morphology of the $MnPS_3$ is analyzed by scanning electron microscopy (SEM) and the chemical composition was determined by EDEX before and after intercalation process. Fig. 12(a) represents the SEM images of the pure $MnPS_3$ materials. Fig. 12(b) shows the structure morphology of $MnPS_3$ after intercalation with pyridine. The images show the layers piled up on

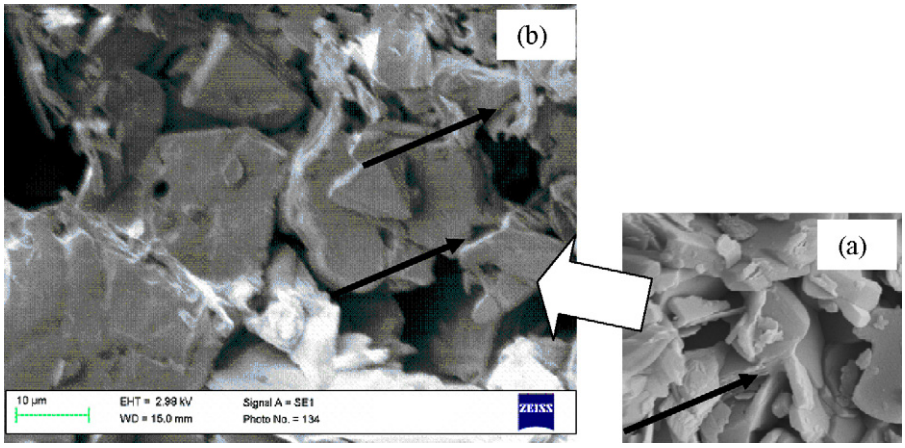

Fig. 12. SEM for $MnPS_3$ made at 650 °C under slow heating rate (0.1 °C/m) for 6 days: (a) before intercalation and (b) after intercalation with pyridine. Arrow refers to flakes of the $MnPS_3$ layers. It has the same layer structure before and after intercalation.

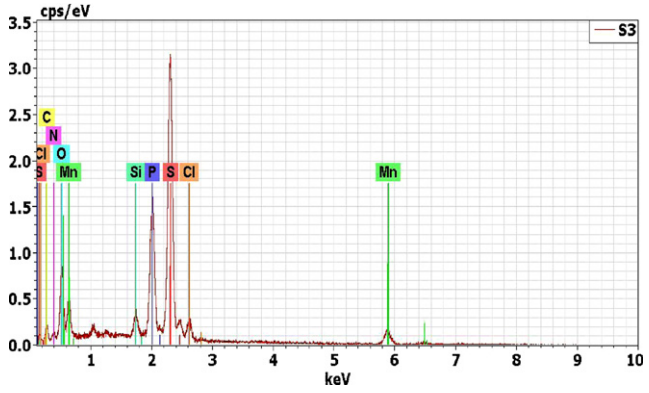

Fig. 13. EDEX spectrum of the intercalated compound $Mn_{1-x}PS_3(C_5H_5N)_{2x}(H_2O)_y$.

each other. This observation indicates that the layered structure of $MnPS_3$ has not been affected by the intercalation process conditions (stirring, solvents, distilled water and HCl, and temperature). EDEX analysis indicates the presence of S, Mn, O, P, N, C, Cl, C, and Si elements in the intercalated compound $Mn_{1-x}PS_3(C_5H_5N)_{2x}\cdot(H_2O)_y$, as can be seen in Fig. 13. The silicon is supposed to be arising from the microscope slide; oxygen comes from the water during experiment and from the water vapor in air; and chlorine (Cl) comes from the hydrochloric acid (HCl) during intercalation process in which conversion of pyridine into pyridinium is possible: pyridine + $H_3O^+ \leftrightarrow pyH^+ + OH^-$ [13,28]. Accordingly, pyH^+ can react with HCl to form pyridinium chloride (pyH^+Cl^-). Therefore, Cl is detected by EDEX.

3.7. Infrared (IR) measurements

The IR spectrum of pure $MnPS_3$ shows the presence of the stretching band at 570 cm^{-1} for $\nu(PS_3)^2$, as shown in Fig. 14. The IR measurements show an evidence of the presence of complete intercalation (Fig. 15). The spectrum of the intercalated materials show the splitting of $\nu(PS_3)^{2-}$ asymmetric stretching band of pure $MnPS_3$ into two or three strong sharp absorption frequencies in the range 550–620 cm^{-1} [18–20,33,34]. The IR spectrum are identical to that obtained for $MnPS_3$ intercalated with pyH^+ [14], where the spectra show strong characteristic ring frequencies of the pyH^+ and with presence of bands that can be attributed to pyH^+ or pyridine species. The pyH^+ could convert into pyridine and vice versa [26,35]. Generally, the two or three absorptions of intercalates occurring at around 620–550 cm^{-1} originate from the splitting of 570 cm^{-1} of pure host (e.g. $MnPS_3$), which reflects the presence of intralayered Mn^{2+} ion vacancies [29,32]. Obviously, the inserted compound should be in the cationic form to compensate positive charge of Mn^{2+} ions leaving from the intralayered centre and maintain charge balance of the intercalate. The broad band at about 3420 cm^{-1} is for normal hydroxyl group stretch, which is mainly from water [36]. The broadening is due to hydrogen bonding with other hydroxyl groups. The IR spectrum shows evidence of pyridine bands. As known, pyridine is an aromatic compound. The aromatic C–H stretch appears at 3100–3000 cm^{-1} as shown in Fig. 15. There are aromatic C–C stretch bands (for the carbon–carbon bonds in the aromatic ring) at about 1500 cm^{-1}. The C=C, double bonds appear as medium to strong absorptions in the region 1650–1450 cm^{-1}, as shown in Fig. 15. Two weak bands are caused by bending motions involving carbon–hydrogen bonds. The bands for C–H bends appear at approximately 1000 cm^{-1} for the in-plane bends and at about 675 cm^{-1} for the out-of-plane bend [37].

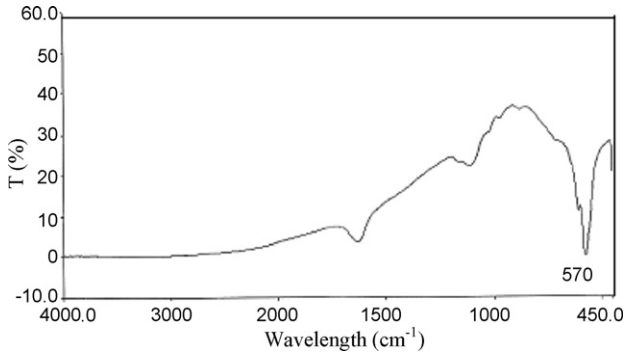

Fig. 14. IR spectrum of pure $MnPS_3$.

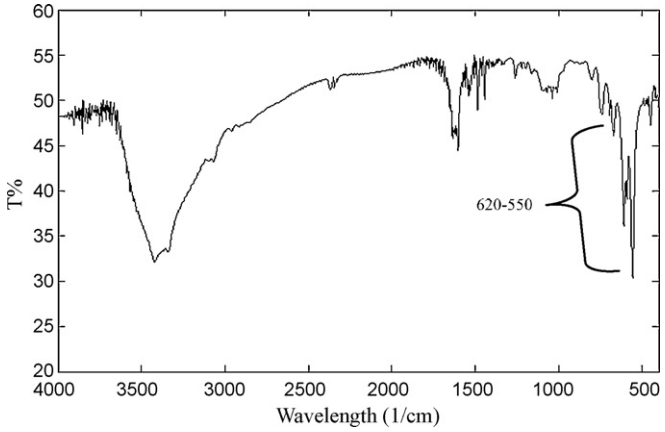

Fig. 15. IR spectrum of the intercalate $[Mn_{1-x}PS_3[pyr_{2x}(H_2O)_y]$.

4. Conclusion

The intercalation of pyridine with semiconductor layered crystalline of $MnPS_3$ under specific conditions reveals that:

1. Three crystalline phases appeared together as confirmed by XRD analysis. This behaviour reflects the elasticity of interlayer gap of $MnPS_3$.
2. The most interesting feature is the phase transformation, which occurs in open atmosphere at room temperature without any other external factors. There was a complete phase transformation of the 0 0 1′ phase and 0 0 1″ after one day. Then the 0 0 1″ phase transformed into 0 0 1′ phase again.
3. The crystallite size of different phases was estimated from XRD. It was observed that the phase transformation greatly affect the crystallite size: the largest crystallite size up to 440 nm for 0 0 1′ phase and the smallest for d7 phase, whereas for the 0 0 1″ phase is in the range of 30–100 nm.
4. The magnetic properties, i.e. saturation magnetization Ms of the $MnPS_3$ are affected to the pyridine intercalation.

References

[1] R. Clement, M.L.H. Green, J. Chem. Soc., Dalton Trans. 10 (1979) 1566.
[2] T. Coradin, A. Coupe, J. Livage, J. Mater. Chem. 13 (2003) 705.
[3] X. Zhang, H. Zhou, X. Su, X. Chen, C. Yang, J. Qin, M. Inokuchi, J. Alloys Compd. 432 (2007) 247–252.
[4] R. Clement, O. Garnier, J. Jegoudez, Inorg. Chem. 25 (9) (1986) 1404.
[5] T. Coradin, R. Clement, Chem. Mater. 8 (1996) 2153.
[6] N. Mirabal, V. Lavayen, E. Benavente, M.A. Santa Ana, G. Gonzalez, Microelectron. J. 35 (2004) 37.
[7] A.M. Fogg, V.M. Green, D. O'Hare, Chem. Mater. 11 (1999) 216.
[8] I. Lagadic, P.G. Lacroix, R. Clement, Chem. Mater. 9 (1997) 2004.
[9] T.A. Kerr, H. Wu, L.F. Nazar, Chem. Mater. 8 (1996) 2005.
[10] M. Lira-Cantu, P. Gomez-Romero, J. Electrochem. Soc. 146 (1999) 2029.

[11] J.G. Qin, C.L. Yang, K. Yakushi, Y. Nakazawa, K. Ichimura, D.Y. Liu, Synth. Met. 85 (1997) 1673.
[12] C.L. Yang, X.G. Chen, J.G. Qin, K. Yakushi, Y. Nakazawa, K. Ichimura, J. Solid State Chem. 150 (2000) 281.
[13] R. Clement, J.J. Girerd, H. Badarau, J. Inorg. Chem. 19 (1980) 2852.
[14] J.P. Audiere, R. Clement, Y. Mathey, C. Mazieres, Physica B 99 (1988) 133.
[15] R. Clement, M. Doeuff, C. Gledel, J. Chim. Phys. 85 (1988) 1053.
[16] A.A. El-Meligi, Mater. Chem. Phys. 84 (2–3) (2004) 331–340.
[17] A.A. El-Meligi, J. Mater. Sci. Technol. 22 (2) (2006).
[18] E. Prouzet, G. Ouvrard, R. Brec, Mater. Res. Bull. 21 (1986) 195.
[19] L. Silipigni, G. Di Marco, G. Salvato, V. Grasso, Appl. Surf. Sci. 252 (2005) 1998–2005.
[20] R. Clement, in: J.E. Mark, C.Y.C. Lee, P.A. Bianconi (Eds.), Hybrid Organic–Inorganic Composites, Symposium Series, American Chemical Society, Washington, DC, 1995, chapter 4, p. 29.
[21] X. Zhang, X. Chen, X. Su, C. Yang, J. Qin, M. Inokuchi, J. Solid State Chem. 177 (2004) 2014.
[22] H. Zhang, J.F. Banfield, Chem. Mater. 14 (2002) 4145.
[23] H. Hsiang, S. Lin, Mater. Chem. Phys. 95 (2006) 275–279.
[24] X. Chen, C. Yang, J. Qin, K. Yakushi, Y. Nakazawa, K. Ichimura, J. Solid State Chem. 150 (2000) 285.
[25] J. Qin, C. Yang, K. Yakushi, Y. Nakazawa, K. Ichimura, Solid State Commun. 100 (1996) 427.
[26] T. Miyazaki, K. Ichimura, S. Matsuzaki, M. Sano, J. Phys. Chem. Solids 54 (9) (1993) 1023.
[27] M. Hangyo, S. Nakashima, A. Mitsuishi, K. Kurosawa, S. Sato, Solid Sate Commun. 65 (1988) 419.
[28] R. Clement, L. Lomas, J.P. Audiere, Mater. Chem. 2 (1990) 641, 1990.
[29] P.A. Joy, S. Vasudevan, J. Am. Chem. Soc. 114 (1992) 7792.
[30] R. Schollhorn, H.D. Zagefka, Angew Chem. Int. Ed. Engl. 16 (1977) 199.
[31] D. Peng, S. Beysen, Q. Li, J. Jian, Y. Sun, J. Jiwuer, Particuology 7 (2009) 35.
[32] B.D. Cullity, Introduction to Magnetic Materials, Adison-Wesley Publishing Company, 1972, chapter 7, p. 207.
[33] Y. Mathey, R. Clement, C. Sourisseau, G. Lucazeau, Inorg. Chem. 6 (1982) 2773.
[34] C. Sourisseau, J.P. Forgerit, Y. Mathey, J. Solid State Chem. 49 (1983) 134.
[35] R.H. Friend, A.D. Yoffe, Adv. Phys. 36 (1987) 94.
[36] J. Coates, in: R.A. Meyers (Ed.), Interpretation of Infrared Spectra, A Practical Approach in Encyclopedia of Analytical Chemistry, John Wiley & Sons Ltd., 2000, pp. 10815–10837.
[37] N.B. Colthrup, L.H. Daly, S.E. Wiberley, Introduction to Infrared and Raman Spectroscopy, Academic Press, San Diego, 1990, CA, pp. 1–73.